Space Shuttle and Launch Pad Computational Fluid Dynamics Model for Lift-off Debris Transport Analysis

by

Sam Dougherty^
Jeff West, Alan Droege, and Josh Wilson*
Peter A. Liever and Matthew Slaby!

17th Annual Thermal and Fluids Analysis Workshop (TFAWS 2006)

Abstract

This paper discusses the Space Shuttle Lift-Off CFD model developed for potential Lift-Off Debris transport for return-to-flight. The Lift-Off portion of the flight is defined as the time starting with Tanking of propellants until 'Tower Clear', approximately T0+6 seconds, where interactions with the Launch Pad cease. A CFD model containing the Space Shuttle and Launch Pad geometry has been constructed and executed. Simplifications required in the construction of the model are presented and discussed. A body-fitted overset grid of up to 170 million grid cells was developed which allowed positioning of the Vehicle relative to the Launch Pad over the first six seconds of Climb-Out. The CFD model works in conjunction with a debris particle transport model and a debris particle impact damage tolerance model. These models have been used to assess the interactions of the Space Shuttle plumes, the wind environment, and their interactions with each other and the Launch Pad and their ultimate effect on potential debris during Lift-Off.

Introduction

On January 16, 2003, the 28th flight of the Shuttle Columbia was launched from Kennedy Space Center (KSC). This was the 113th mission of the Shuttle Program, designated STS-107. At 81.7 sec after launch, when the Shuttle was at about 65,200 ft and traveling at Mach 2.46 (1,650 mph), a large piece of hand-crafted insulating foam came off the forward bipod area where the Orbiter attaches to the External Tank (ET). At 81.9 sec, the foam struck the leading edge of Columbia's left wing[1]. There was a breach of the wing, eventually destroying the wing during reentry and causing the loss of Columbia and its crew on February 1, 2003.

The need to determine the possible size, speed, impact location, and impact energy of debris led NASA and the Columbia Accident Investigation Board (CAIB) to use Computational Fluid Dynamics (CFD) techniques to analyze the event[2, 3]. The Space Shuttle Program also undertook the effort of identification and control of every possible source of debris liberation. The OVERFLOW CFD program[4] and chimera grid approach had been in use at NASA/JSC to simulate the flow over the integrated Space Shuttle Launch Vehicle (SSLV) for over 16 years.

* NASA/MSFC, Huntsville, AL
^ Technical Fellow, ERC, Inc., MSFC, Huntsville, AL
! CFDRC, Huntsville, AL

These simulations were refined in support of the return-to-flight effort. Through the leadership of the authors of Reference 2, significant geometric detail was added to the Vehicle CFD model such that the model consists of over 35 million grid cells. Steady-state CFD calculations were performed at several flight conditions duplicating the STS-107 ascent trajectory. The CFD simulations provide not only the aerodynamic forces on the Vehicle but also a flow field for the ballistic integration of possible debris flight trajectories.

In February 2004, as part of the return-to-flight effort, NASA/MSFC was assigned the portion of SSLV flight regime from the beginning of propellant Tanking up to the time when the Vehicle has cleared the Launch Tower. The active mechanisms for possible debris transport are gravity, Ground Winds, integrated propulsion system exhaust plumes and interaction of these mechanisms with Ground Facility structures. A new CFD model was constructed that included the pre-existing SSLV model from NASA/JSC augmented with all of the relevant Launch Pad Ground Facility structure. Point mass debris tracing was used for the aerodynamic transport of possible debris particles in this timeframe. This paper discusses the Space Shuttle Lift-Off CFD model developed for Lift-Off Debris Transport Analysis (DTA) supporting return-to-flight and continuing Space Shuttle operations.

Debris Analysis and Risk Mitigation

Aggressive debris mitigation and debris risk assessment have been carried out by NASA and its contractors supporting Space Shuttle return-to-flight. Debris environment analysis for Lift-Off and Ascent follows a continuous improvement path to support all remaining Space Shuttle flights through International Space Station Assembly Complete. The Space Shuttle Program undertook mitigation of potential debris release and characterization of what debris might still be liberated on the basis of mass, material, density, shape, location and time of release. Potential debris items were compiled into a database and characterized as either expected or unexpected by design or process controls[5].

The most difficult requirement, derived from the greatest debris threat, for the Lift-Off Debris Transport Analysis to address is the ability to predict the velocity and direction debris might take if it is caught in an exhaust plume and turns back upward towards the SSLV. This is a probabilistic problem inasmuch as uncertainties in assumptions and models must be known and dispersions in the important transport variables must be understood.

Foreign Object Debris (FOD) control at Shuttle Launch Complex 39 Pads A and B is a prime concern and a responsibility for all who work there. In addition, corrosion from SRB exhaust products and the salt mist from the ocean incessantly weaken the structure. Rust flakes, bolts, nuts, and washers and other damaged hardware must be removed by continual Pad refurbishment and rigorous corrosion mitigation discipline. A disciplined mitigation effort was accomplished at Pad B before the return-to-flight Missions STS-114 and 121 and is in progress at Pad A before launches resume there.

FOD as well as most systems elements liberated debris at the Pad is characterized as unexpected debris. However, Facility rust and scale at the target mitigation limit of 0.014 lbm (approximately the size of a U.S. quarter) are characterized as expected debris. The MSFC Propulsion Systems Engineering and Integration Office is responsible for determination of the Lift-Off debris environment. MSFC Engineering developed the Lift-Off CFD model and is performing the Lift-Off DTA.

The Lift-Off CFD model requirements are extensive. The model shall be applicable to the Tanking period prior to launch, while ice or other potential debris might fall on the Vehicle. It must be applicable to Main Engine Start, at Solid Rocket Booster Ignition, and during Climb-out past 'Tower Clear', where vibration and plume blast may result in the liberation of debris that can impact the Vehicle.

The Nominal Launch Sequence

Shuttle launch operations are to be simulated beginning with the Tanking period when cryogenic propellants are on-board and dropped to the SSMEs for chill-down and recirculation. Ice formation, which depends on temperature, humidity and Ground Winds, presents the threat of falling ice debris from this time forward. Ice may come from the External Tank (ET), feedline bellows and brackets, aft fittings, and Main Engines.

At ~ T0 – 6 sec, the Space Shuttle Main Engines (SSMEs) are started. By ~ T0 – 2 sec the SSMEs have reached 100 % rated power level. SRB Ignition Command is issued at T0 at which time the SRB holddown explosive fasteners are fired and the T0 umbilicals are retracted. The T0 umbilicals consist of the LO2 and LH2 Tail Service Mast (TSM) umbilicals on the Mobile Launch Platform (MLP) and the GH2 Vent Line at the ET Intertank. The time ~ T0 + 0.3 sec is the moment that the SSLV begins to rise as it is the time that the SRBs have attained full thrust. During the climb-out period, the SSLV is under the threat of 'Pad debris' that may be blown upward as a result of plume interactions with Ground structures. The SSLV is under the threat of falling debris that can fall from either the SSLV or Pad structures above. The SSLV vibration, acoustics, and ignition overpressure may excite debris on either the SSLV or the Pad to be liberated at any time after SSME Start.

There is therefore a time during SSLV Climb-out after which the interactions with Launch Facility structures no longer can have an influence on the SSLV debris environment. Upward-traveling debris particles can no longer overtake the SSLV, and falling particles from the highest locations on the Launch Access Tower can no longer have a possible trajectory to the SSLV. We define this ending time for Lift-Off DTA to be 'Tower Clear'. It is approximately when the SRB aft skirt aft extremity is higher than the top of the Fixed Service Structure (FSS) Access Tower and is at ~ T0 + 6 sec.

We chose to perform CFD simulations using steady state time slices, referred to as Cardinal Points (CardPts). The Cardinal Points are shown in Table I and were chosen based on knowledge of key events in the time sequence. The first, CardPt 1, can be any time when propellants are loaded and the Vehicle and SSMEs are fully chilled and there is ice/frost formation. CardPt 2 is after the three SSMEs have attained 100 % rated thrust level. CardPt 3 is reserved for future analyses of the SRB ignition transient (not a part of the present steady-state simulations).

Table I. CFD Cardinal Points

Wind Speed	Time	6.7 knots								20.1 knots								33.5 knots							
Wind Direction	sec from T0	45	90	135	180	225	270	315	360	45	90	135	180	225	270	315	360	45	90	135	180	225	270	315	360
CardPt1	prior to -6.0	X	X	X	X	X	X	X	X	X	X	X	X	X	X	X	X	X	X	X	X	X	X	X	X
CardPt2	-2.0	X	X				X	X	X	X	X				X	X	X	X	X				X	X	X
CardPt3	-	Reserved for Later Use																							
CardPt4	0.3	X	X				X	X	X	X	X				X	X	X	X	X				X	X	X
CardPt5	1.9								X																
CardPt6	3.0								X																
CardPt6a	3.0								1																
CardPt7	4.0								X																
CardPt8	5.0								X																
CardPt9	6.0								X																
CardPt9a	6.0								1																

Note 1: Cardinal Points 6a and 9a used forward flight velocity from the STS-113 BET.

CardPt 4 is at the moment of lift-off, at ~ T0 + 0.3 sec. CardPt 5 is at a critical time in the plume flow transient when the three SSME plumes are fully contained in the SSME exhaust hole in the MLP but the two SRB exhaust plumes begin to impinge on MLP structure, at ~ T0 + 1.9 sec. As the Vehicle climbs, the SRB plumes begin to impinge on the SRB holddown posts and haunches starting at ~ T0 + 1.5 sec. This SRB plume impingement continues on but begins to abate by ~ T0 + 4 sec as the Vehicle gains more height. The impingement pattern in the SRB exhaust holes changes during the 1.5 - 4 sec interval because the Vehicle is rising and also because it drifts in the Vehicle body axis plunging direction, Pad North (Vehicle $-Z_T$ coordinate direction), due to the thrust vector of the SSMEs.

A new flow phenomenon is initiated at ~ T0 + 3 sec as the SRB plumes are larger than the width of the SRB exhaust holes and begin to spill out onto the MLP Deck. Gross SRB plume spillage and impingement on the flat Deck continues on until well after 'Tower Clear'. This flow condition is captured in CardPt 6.

At ~ T0 + 4 sec, there is considerable interaction among the five exhaust plumes and the Facility structures, but the plumes from the two lower SSMEs begin to impinge on the TSMs and spill out of the SSME exhaust hole. This flow condition is captured in CardPt 7.

Simply continuing with the climb-out phase on past 'Tower Clear' at even 1 sec intervals, CardPts 8 and 9 have the Plume–Facility interactions at T0 + 5 sec and 6 sec, respectively, with 'Tower Clear' at ~ T0 + 6 sec.

Lift-Off Debris Transport Analysis

The Lift-Off Debris Transport Analysis process is illustrated in Figure 1. The analysis begins with a CFD simulation of the flowfield about the Vehicle and related Ground Structure. The prediction is at a given time Pre-launch, during Lift-Off or Ascent flight and is a quasi steady-flow solution representing an instant in time. The time slice for the CFD analysis is referred to as a Cardinal Point (CardPt).

Initial debris locations and release velocity vectors are known or estimated. The debris is modeled as a point mass where just its material and density, mass m, drag coefficient, C_D, cross-section reference area, A_{ref}, and therefore its ballistic number, BN are required. A debris transport trajectory integration program, ***debris***[6], computes the trajectory of the debris particle through the CFD flowfield from the point of release either to impact or miss the SSLV.

Impacts are detected and characterized as to their impact relative velocity, kinetic energy, and angle by the ***dprox***[7] program. Many debris particles of different size and shape may be released as point masses into a given CFD flowfield and the maxima in impact kinetic energy or angle or velocity sorted in a given impact zone on the SSLV. Many such sorts for the impact quantity maxima make up the potential SSLV debris impact environment.

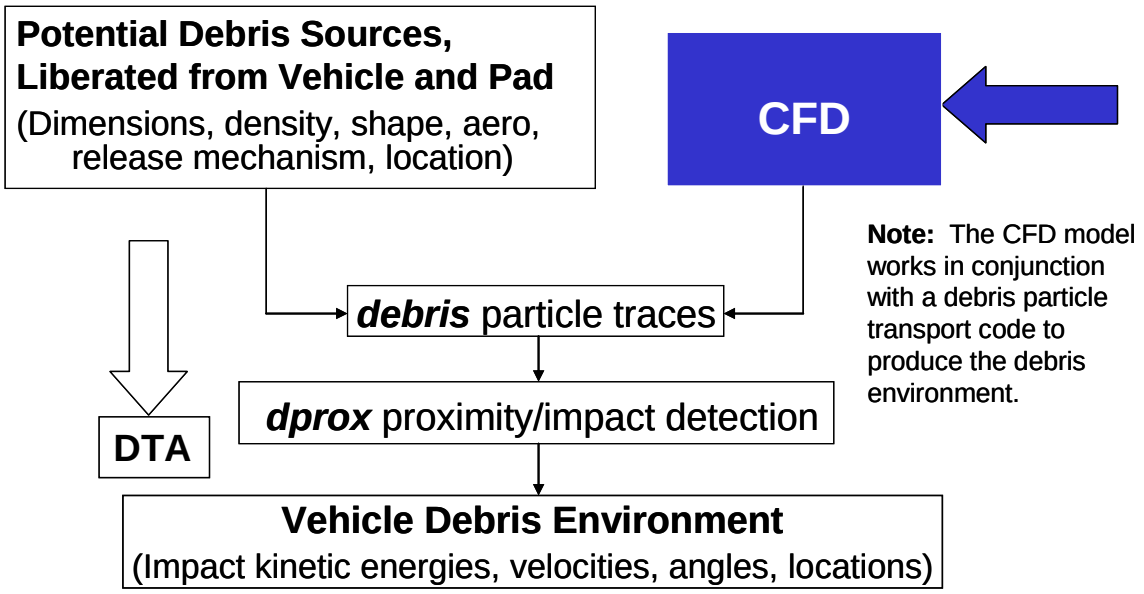

Figure 1. The Debris Transport Analysis Process

AnalysisTools

The OVERFLOW CFD program is used to simulate the Lift-Off flowfield because the ***debris*** and ***dprox*** tools were developed to use the CFD flowfield from this particular CFD solver. Having a full existing tool suite and a common approach for Lift-Off and Ascent Debris Transport Analysis made it a pragmatic decision to use the OVERFLOW program. The time required to complete the reconstruction of an equivalent tool suite based on another CFD program was judged to be prohibitive. The only risk associated with this decision is that OVERFLOW uses a 'density-based' algorithm and had only recently been upgraded to include a preconditioned formulation for low-Mach number accuracy. It was unknown whether this formulation was capable of robustly and accurately simulating this problem which depends on robust and accurate flow-field predictions with significant portions of the same simulation having Mach numbers ranging from 0.01 to 6.

Previous CFD models[8, 9] of the SSLV On-the-Pad have been only Pre-launch. They were of 2D section cuts through the Vehicle and of an External Tank (ET) - Solid Rocket Booster (SRB) 3- D half-model with Pre-launch winds and humidity influences on the ET chill effect and utilized the Rockwell International Unified Solution Algorithms code[10]. There have been recent wind tunnel tests measuring Vehicle integrated force and moment coefficients from pressure-area loads due to

Pre-launch Ground Winds[11]. This and prior[12, 13] wind tunnel data are being used to support validation of the Lift-Off CFD model.

Objective and Approach

The objective was to develop a Lift-Off CFD model in which the transport of potential lift-off debris could be evaluated. This was in order to provide impact data from which debris damage tolerance assessments could be made as to location and severity of debris impacts. Rapid response was needed to support return-to-flight. There were several important simplifications made in order to be responsive.

Simplifications

The simplifications are rank-ordered in what is believed to be the order of their importance to Lift-Off DTA, and priorities for continuous improvements were set based on this rank order.

The ***first simplification*** was to use the quasi steady state approximation.

It is not yet possible to simulate using CFD the SSLV lift-off transient in a time-accurate mode and include the necessary geometric detail. The SSLV moves with respect to the Launch Pad, various components articulate and power setting changes occur with the SSLV in flight as a function of time. Therefore we resorted to quasi-steady simulation using the CardPts and Ground Wind dispersions within a given CardPt. Dispersions cover an envelope of possible Ground Winds day to day (see Table 1). This decision largely defined the required number of CFD simulations which wound up being sixty-one.

The time scale between the release of a piece of debris and its impact on the SSLV is on the order of milliseconds when the Vehicle is flying at supersonic speeds (as in the case of the STS-107 foam impact). The quasi steady-state approximation for the CFD flow field is justified in that case. However, the time for debris being released at Lift-Off, being accelerated by gravity and/or interaction with the propulsive flows and Ground Facility, and coming back to an impact on the SSLV may be on the order of seconds. The SSLV will have moved with respect to the Facility during that elapsed time from the debris release to its impact. For Lift-Off Debris Transport Analysis, the quasi steady-state approximation for the flow field is clearly not justified.

We propose that by selecting a large enough number of time slices (CardPts) it is possible to represent the real transient problem. This is an approach that may bound the debris transport phenomena. Comparing CFD results with launch imagery from many flights has been the verification approach taken to try to verify that we have enough CardPts and that we have included sufficient geometric detail. But this approach is no substitute for striving to work the transient problem in the future based on our continuing improvement philosophy stated above.

The ***second simplification*** was to use a single fluid specie, air as a perfect gas, with $\gamma = 1.4$. This is the working fluid everywhere; hot air at high velocities is used to simulate all exhaust plumes. Thus, the CFD model approximates the plume gaseous composition and neglects completely the condensed-species particulates in the SRB exhaust plumes. State-of-the-art SRB plume simulations[14] (single plume, axisymmetric) include the particulate flow, but two-phase flow simulation is a complexity that would have taken too long to implement in this 3-D model. This simplification still provided reasonable plume jet velocities and pitot impingement pressures, but left out ~ 40 % of the SRB exhaust mass flow (the condensed-species particulates).

Real gas plume simulations have been evaluated for Space Shuttle Ascent flight conditions[15] using OVERFLOW with the conclusion that γ = 1.4 plumes with MW = 29.0 would provide adequate aerodynamic simulation with the plume expansion (and blockage effect) at altitude based on the Orbiter surface c_p.

For the Lift-Off regime, accurate simulation of shocks, expansions, and mixing has considerably different modeling requirements[16] than do plumes at altitude that are underexpanded. Real gas thermal and fluid transport properties must be preserved to retain all of the plume energy properly and capture the aspiration, impingements and reverse flows accurately. In the spirit of continuing improvement, this simplification should also be amended.

The ***third simplification*** was to de-feature some of the Facility structure surface details. For example, the Fixed and Rotating Service Structures were neglected. The SRB exhaust holes in the Mobile Launch Platform (MLP) were significantly de-featured, but retain the basic geometrical shape of the actual hardware. What results is considered to be a first-order geometry representation for effects of SRB plume impingement and recirculation and was constructed. Even with aggressive de-featuring to manage the size of the CFD grid, some CardPts contained up to 170 million cells.

Unstructured grid technology offers the flexibility to cluster more grid points where needed and less where they are not needed. Converting to a CFD solver that supports unstructured grids would allow the addition of more Ground structure features in a continuous improvement path.

The ***fourth simplification*** was to neglect the Sound and Ignition Overpressure Suppression Water bags and sprays. This decision eliminated > 1,000,000 gpm Sound Suppression Water and steam flow from the total flow. The water sprays are below the MLP elevation considered most important for debris sources at Lift-Off and Post-Liftoff, and a blocking filter was used in ***debris*** to restrict any debris sources coming from below the water sprays locations. Post-Liftoff sprays come on for acoustic noise suppression at the top Deck of the MLP after ~T0 + 3 sec. The possible effects that energy extraction from the plumes and volume expansion from flashing of the water to steam could have on plume entrainment and/or rebound of debris particles was not included because it was judged to be small.

The ***fifth simplification*** was a simple slug flow profile Ground Wind that did not have the Earth boundary layer effects of vertical wind shear velocity profile and inclusion of the berm effect of the 'Hill' close to the Pad. Ground Winds were simply applied as slug flow dispersions every 45 deg around the compass, at three wind speeds – mean, near 2σ high, and near 3σ high.

This simplification left out the Ground Wind blockage effect of the Fixed Service Structure. This blockage will have an influence on debris transport particle trajectories when the Ground Wind direction is near either 270 deg (from the West) or 90 deg (from the East), but was considered to be small based on the wind tunnel results of Reference 11.

Grid Construction, Vehicle Configuration, and Boundary Conditions

The present model combines the Space Shuttle body-fitted structured grid with a newly constructed body-fitted grid for the MLP and Ground structures. The SSLV model has all protuberances on the ET resolved down to y^+ = 1 and over 80 million grid points including exhaust plume grids. It corresponds to the STS-114 configuration and has 270 multi-block grid blocks. Plume boundary ('start line') conditions are applied at the nozzle exits of the SSMEs and SRBs and are obtained from the JANNAF Standard Plume codes[14]. The SSME nozzle flow definition agrees well with solutions obtained using other codes such as the Finite Difference Navier-Stokes (FDNS) solver[16], for instance.

A detailed Launch Complex 39 Facility CAD model provided the geometry needed for generating the Lift-Off CFD grid model[17]. Integrated with the Launch Facility, the CFD volume grid was as large as 170 million grid cells.

Low Mach Number Pre-conditioning

Pre-conditioning was necessary for OVERFLOW code operation at Ground Wind velocities. There is the extreme range in velocities all the way from nozzle exit plume velocities (Mach 6) down to the Ground Wind free stream ambient velocities (Mach 0.01). A separate study[18] was conducted at the start of the Lift-Off DTA effort to verify, validate, and test the low Mach number pre-conditioning extension implemented in the OVERFLOW 2.0s flow solver. The study concluded it was possible to demonstrate good performance of the code down to 0.01 Mach number (ambient wind speed of 6.7 knots on a standard temperature-pressure day) for low-speed steady-flow simulations. This was with the Spalart and Allmaras turbulence model[19] and was demonstrated at *Re* up to 2.5 X 10^7.

The Cardinal Point Cases

Sixty-one individual CFD cases were executed at the operating conditions for nine CardPts, Table I. CardPt cases were selected Pre-launch just before SSME Start (~ - 8 sec) and then basically at 1 sec intervals at ~T0 – 1 sec, ~T0 + 0.3 sec, and T0 + 2, 3, 4, 5, and 6 sec. There were Ground Wind dispersions at 24 wind speed-direction combinations Pre-launch. Three wind speeds were selected – 6.7 kts, 20.1 kts, and 33.5 kts (corresponding to M_{inf} = 0.01, 0.03, and 0.05). These three wind speeds also correspond to the Pad nominal, 2σ, and 3σ dispersed wind speed values. Wind directions selected were every 45 deg around the compass. See Table I for these details.

SSLV flight speed, altitude, and drift, rocket chamber pressures *(Pc*'s), gimbals and elevon deflections were taken from typical mission to the International Space Station flight trajectory data. Two CardPts left out the Ground structures in order to include the Vehicle forward flight velocity, CardPt 6a at T0 + 3 sec and CardPt 9a at T0 + 6 sec. The CFD model includes articulating SSME gimbal angles and elevon surface deflections as they are commanded in flight. These changes in SSLV geometry and times at which they occur are listed for each CardPt in Table II. These schedules were followed closely, not precisely, in the CFD model.

Table II. SSME Gimbal and Orbiter Elevon Deflection Schedules

	Time sec from T0	SSME 1 Gimbal, deg	SSME 2 and 3 Gimbal, deg	Inboard Elevon Defl., deg	Outboard Elevon Defl., deg
CardPt 1	~ - 8	0 yaw, 16 pitch	0 yaw, 10 pitch	0	0
CardPt 2	-2.0	0 yaw, 16 pitch	0 yaw, 10 pitch	0	0
CardPt 3	-	0 yaw, 16 pitch	0 yaw, 10 pitch	0	0
CardPt 4	0.3	0 yaw, 16 pitch	0 yaw, 10 pitch	0	0
CardPt 5	1.9	0 yaw, 16 pitch	0 yaw, 10 pitch	0	0
CardPt 6	3.0	0 yaw, 15 pitch	0 yaw, 9 pitch	1	1
CardPt 6a	3.0	0 yaw, 15 pitch	0 yaw, 9 pitch	1	1
CardPt 7	4.0	0 yaw, 12.5 pitch	0 yaw, 7.5 pitch	3	3
CardPt 8	5.0	0 yaw, 12.5 pitch	0 yaw, 7.5 pitch	5	5
CardPt 9	6.0	0 yaw, 12.5 pitch	0 yaw, 7.5 pitch	7	7
CardPt 9a	6.0	0 yaw, 12.5 pitch	0 yaw, 7.5 pitch	7	7

Between T0 + 2.5 sec and T0 + 7.5 sec, the Orbiter elevons are commanded to slew at 2 deg/sec from a preset 0 deg to 9 deg down on the outboard elevons and 10 deg down on the inboard elevons. At T0 + 2 sec the SSMEs, initially set yaw parallel and at 16 deg up for the upper engine (Engine 1) and 10 deg up for the two lower engines (Engines 2 and 3), are commanded to pitch down. By T0 + 4 sec, the upper engine is pitched down 3.5 deg from its initial position to a position of 12.5 deg, and the two lower engines are pitched down 2.5 deg to the 7.5 deg position.

Grid Sequencing and Convergence Criteria

Grid sequencing was used to reduce the computational effort required to arrive at a steady state solution. This was accomplished in a seven-step run recipe wherein the flow around the SSLV and Ground is developed over 1000 iterations without the plumes activated. The second step uses the 'slow-start' feature within OVERFLOW to ramp up the plume boundary condition over 500 iterations and then develop the plumes with an additional 1000 iterations. The first two steps are accomplished on a 4^{th} level sequence grid. Then the solution is refined in step 3 three by running 1000 iterations on sequencing level 3 and so on until the solution is proceeding at 2^{nd} order at grid level 1 on all grids except the SSME grid box, which could be run only at 1^{st} order. Depending on CardPt and wind speed, the total number of iterations required for convergence ranged from 20,000 to 110,000. Grid sequence level 1 is the actual fine-mesh grid. Grid sequence level 2 is 2 X coarser, grid level 3 is 4 X coarser, and grid level 4 is 8 X coarser than the fine grid.

In addition to watching the residuals reduce five orders of magnitude or more, the force and moment coefficient (FOMOCO) integration utilities in OVERFLOW were exercised to watch the integrated Shuttle Vehicle, each Element, and selected structural component FOMOCOs settle to constant values with 'noise' having decayed to a minimum.

The Space Shuttle Vehicle and Launch Facility CFD solutions were performed using a combination of NASA/MSFC Linux clusters and the Columbia SGI Altix system at NASA/ARC. The debris tracing and impact detection and characterization programs were executed on a NASA/MSFC SGI Origin 3900. A full run according to the recipe above could be accomplished in 6 days using 128 cpu's of the Columbia supercomputer. Ground wind dispersion cases were usually started from the solution to another ground wind direction and required about 21 days of 32 cpu's on an Athlon-MP based Linux cluster.

CFD Flowfield Results

For the first time, a full 3-D CFD model has been developed for the Shuttle before and during Lift-Off. The SSLV and Ground Facility models have been combined and the Ground Winds have been modeled. The SSLV is moved in a series of steady state simulations above the Ground to simulate the plume flow interactions with Facility structures and what effects those interactions may have on potential Lift-Off debris transport to impact on the SSLV.

In Figure 2, which corresponds to CardPt 1, the wind originates from the East and wraps around the Vehicle, causing local areas of flow separation and recirculation that could affect debris trajectories. The downstream side of the SSLV is almost completely separated flow as shown by the velocity vectors and synthetic oil flow patterns in Figure 2. Two independent sets of experimental data [11-13] exist for the wind-induced forces on the SSLV on the Launch Pad. In Figure 3, the data sets best corresponding to the CFD model geometry, i.e., without the Fixed and

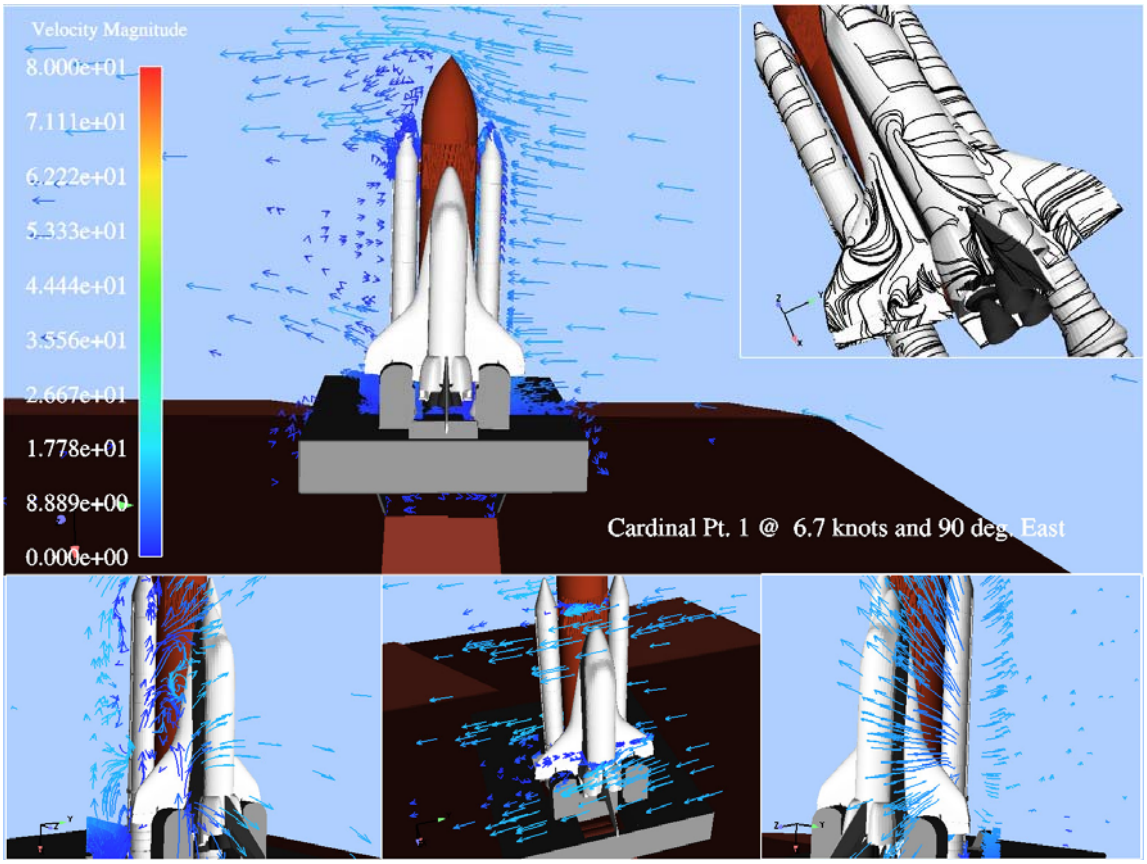

Figure 2. Flow field predicted from CardPt 1 with wind speed of 6.7 knots and wind direction of 90 degrees (from the East).

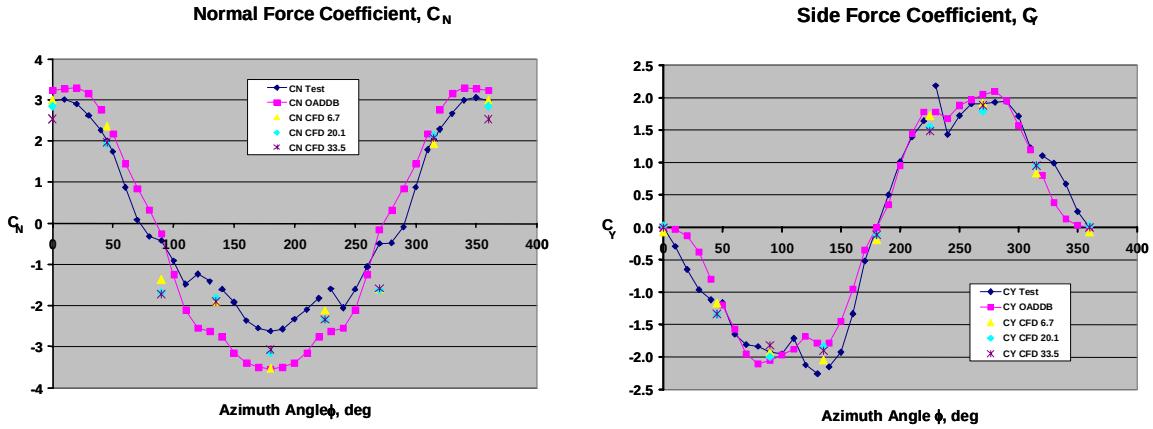

Figure 3. Normal and side force coefficients computed from CartPt 1 compared to two independent sets of experimental data.

Rotating Service Structures (FSS and RSS, respectively) are compared to the normal and side force coefficients computed from CardPt 1 from all wind speeds and directions. The computed force coefficients reasonably replicate the experimental data in both value and nature of response to different wind directions. While this result falls far short of validating the predicted wind interactions with the SSLV and Ground geometry, it does represent one important component of a rigorous validation argument.

Figure 4 shows the predicted wind patterns for CartPt 2, the case where only the SSMEs are operating. In contrast to CardPt 1 flow patterns, the presence of the aspiration from the SSME plumes radically reduces the separated flow volume. Velocity vectors in Figure 4 indicate a general downward flow direction imparted to the flow localized around the SSLV. Synthetic oil flow patterns illustrate the influence of the SSME plume aspiration near the SSLV body. The flow patterns converge on the SSME plumes and could influence debris trajectories towards the base of the SSLV as compared to their trajectories in a CardPt 1 flow field.

To illustrate the consequences of the Second Simplification above, Figure 5 compares a single SSME plume in a near quiescent flow-field computed using finite rate chemistry from JANNAF standard codes to that computed using the OVERFLOW CFD program with the second simplification active. The SSME plume OVERFLOW computations were performed using settings that rendered the algorithm to be first order spatially accurate. This was necessary because the OVERFLOW solver produced IEEE math exceptions when the second order

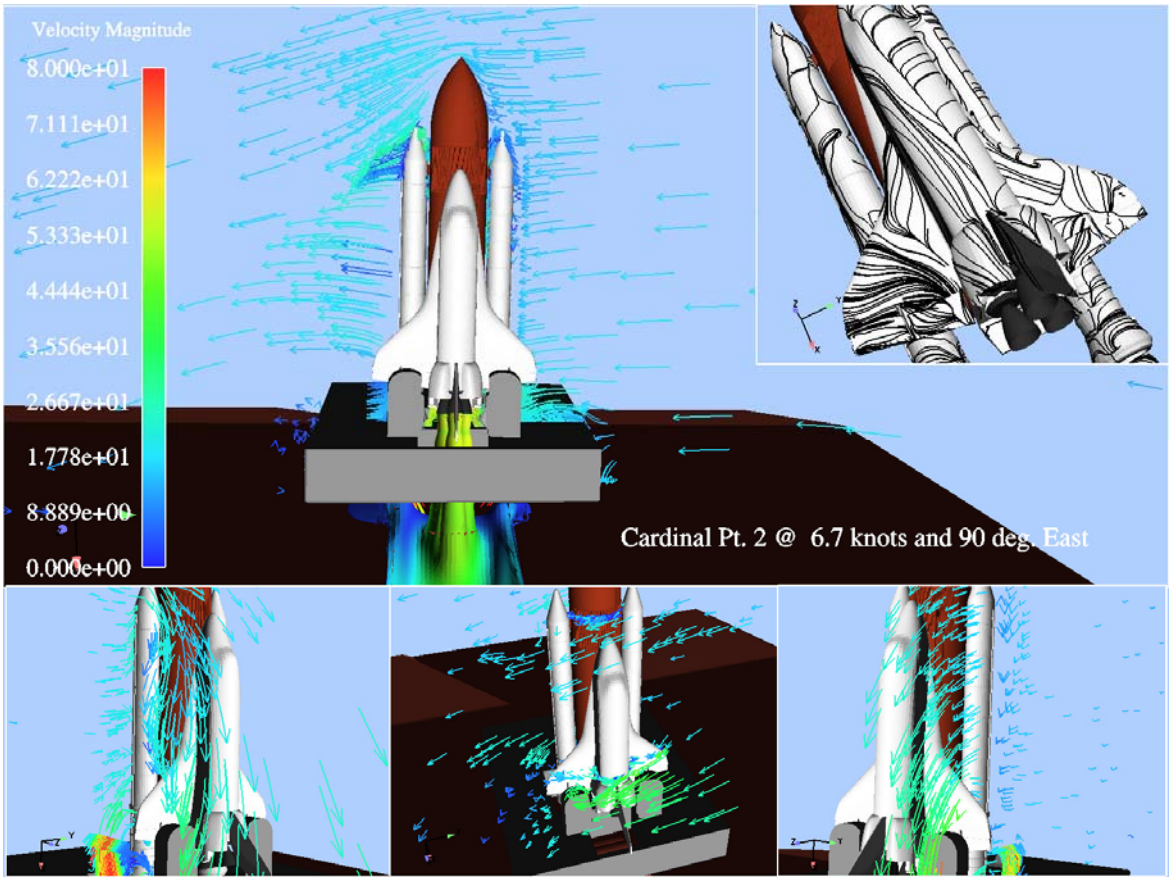

Figure 4. Flow field predicted from CardPt 2 with wind speed of 6.7 knots and wind direction of 90 degrees (from the East).

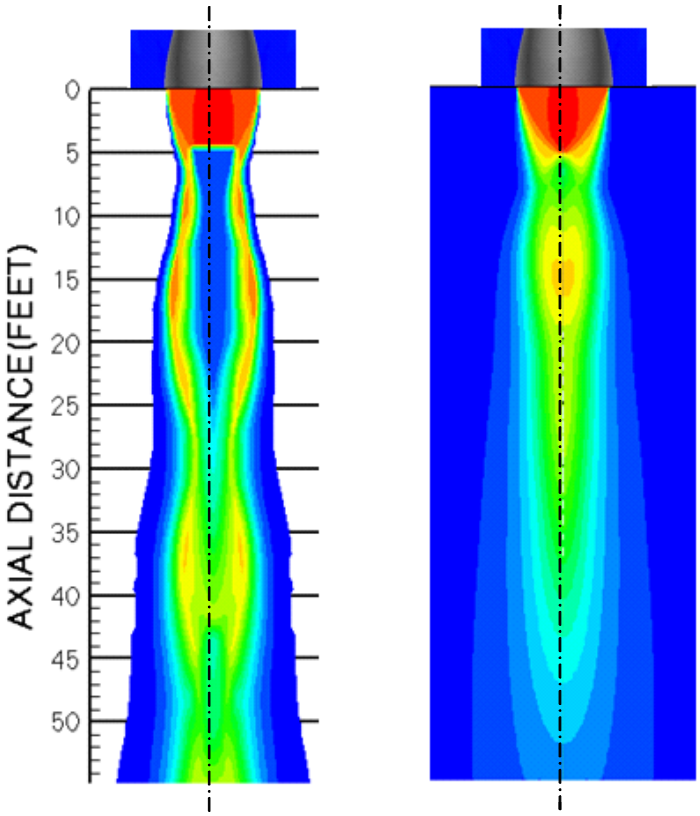

Figure 5. Comparison of single SSME plume computed using finite rate chemistry (left) and computed using OVERFLOW and air as the working fluid (on the right).

algorithm was used. Significant interactions with the developers of the OVERFLOW program over a significant period of time did not result in a solution to this issue. The net result is that the prediction of the SSME plume used in this model degrades with increasing distance from the SSME nozzle exit plane. Figure 5 suggests that the SSME plume prediction is reasonably accurate only to approximately ten feet downstream of the nozzle exit plane. Clearly, this is an aspect of the CFD model that needs to be improved.

Figure 6 shows the predicted wind patterns for CartPt 4, the case where all 5 plumes are activated. In contrast to CardPt 2, the addition of the SRB plumes further strengthens the downward flow and almost completely collapses the separated regions of the flow around the SSLV. The synthetic oil flow patterns indicate a strong downward flow over most of the near body surface, converging towards the plume boundary layer surfaces. These flows towards the Vehicle can influence debris trajectories to impact the SSLV more often and with more energy than gravity and Ground Winds alone.

A comparison of the SRB plume computed from standard JANNAF codes is compared to that computed using OVERFLOW with the second simplification active in Figure 7. For the first 50 feet downstream of the nozzle exit, the two flow fields agree reasonably, but not perfectly. In contrast to the SSME plumes, the OVERFLOW program is capable of robustly simulating the SRB plume using a second order accurate spatial algorithm. Thus the differences between the two plumes in Figure 7 are the appropriate fluid species properties and the lack of the particulate

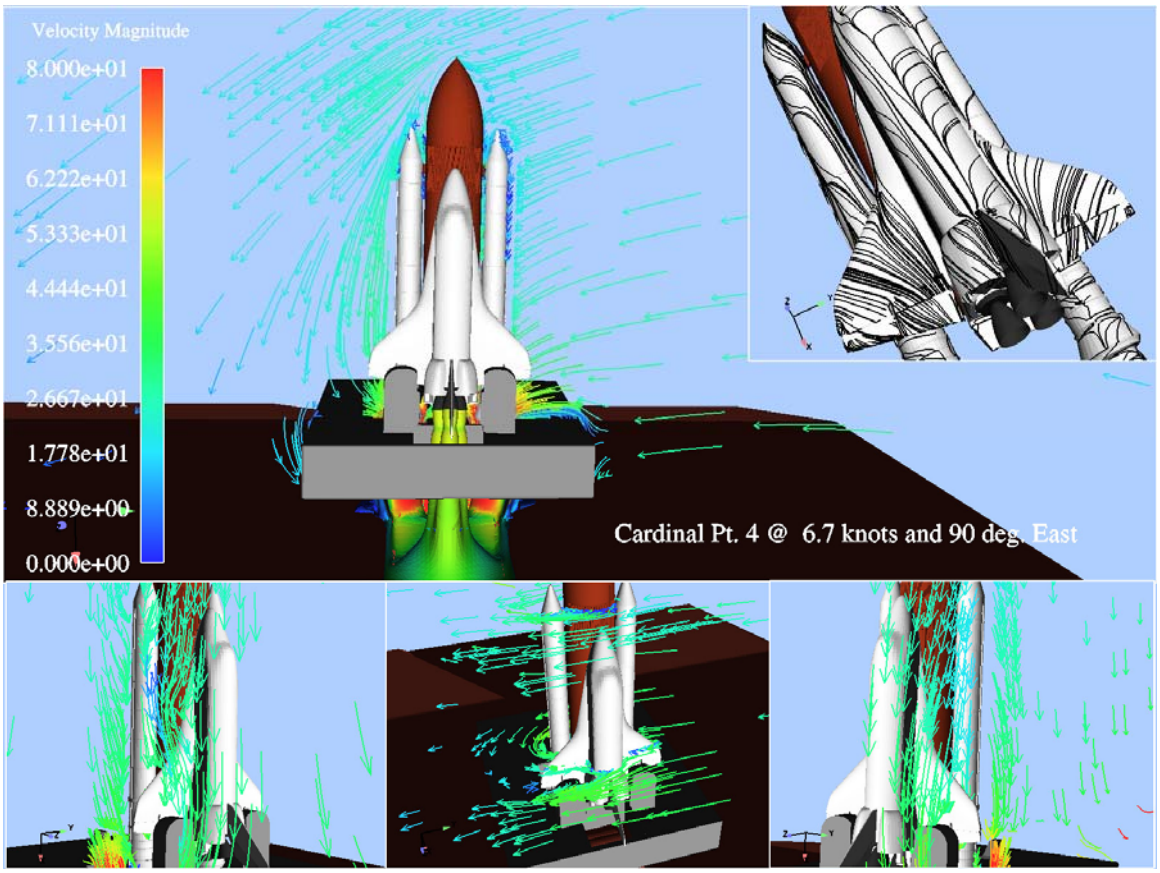

Figure 6. Flow field predicted from CardPt 4 with wind speed of 6.7 knots and wind direction of 90 degrees (from the East).

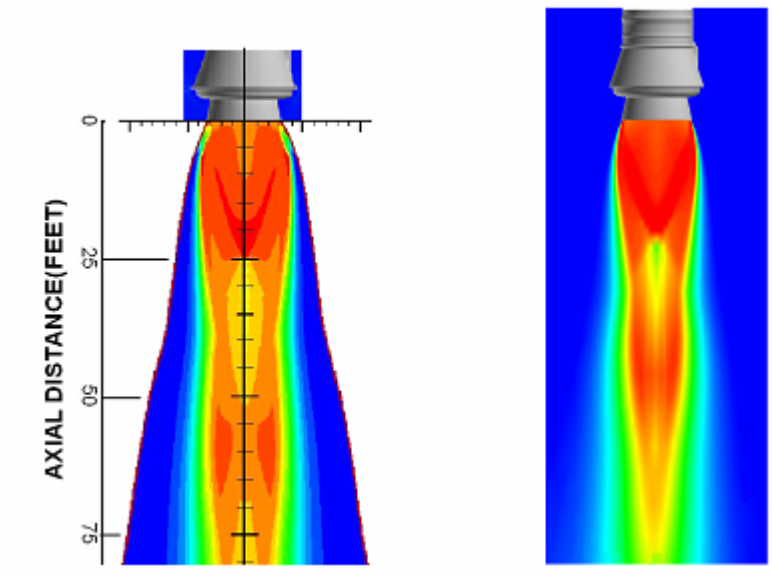

Figure 7. Comparison of SRB plume computed using standard JANNAF codes (left) and the OVERFLOW CFD program (on the right).

model in the OVERFLOW simulation. Both simplifications must be addressed in the spirit of continuous improvement.

Figure 8 illustrates the impact of the plume aspiration on the flow-field, in part a) during CardPt 2 with the just the SSMEs active (upper left view) and in part b), with all five plumes active (upper right view and two lower views). Isosurfaces of constant Mach number around the base of the SSLV illustrate the acceleration and convergence of the flow. Any debris liberated in this region can be exposed to plume aspiration velocities on the order of M = 0.1 or 115 feet per second accelerating the debris towards the Vehicle itself. The streamlines around the Vehicle have the appearance of 'sink flow' in 'potential flow' theory.

When the Vehicle has risen 20-30 ft or so above the Pad, the Vehicle's drift to the North causes an asymmetric SRB plume impingement and recirculation pattern to set in the SRB exhaust hole below. CardPt 5 is definitely into this flow condition with the SSLV height at ~ T0 + 1.9 sec being ~ 27 ft and the drift being ~ 3-4 ft. Figure 9 shows some close-up views of the SRB exhaust plume flow from CardPt 5. On the upper left is the streamline flow close in around the SRB plumes. The streamlines go into the SRB exhaust holes (aspiration). The plume isotherm contour, colored by Mach number up to Mach 1, shows approximately the boundary of the plume

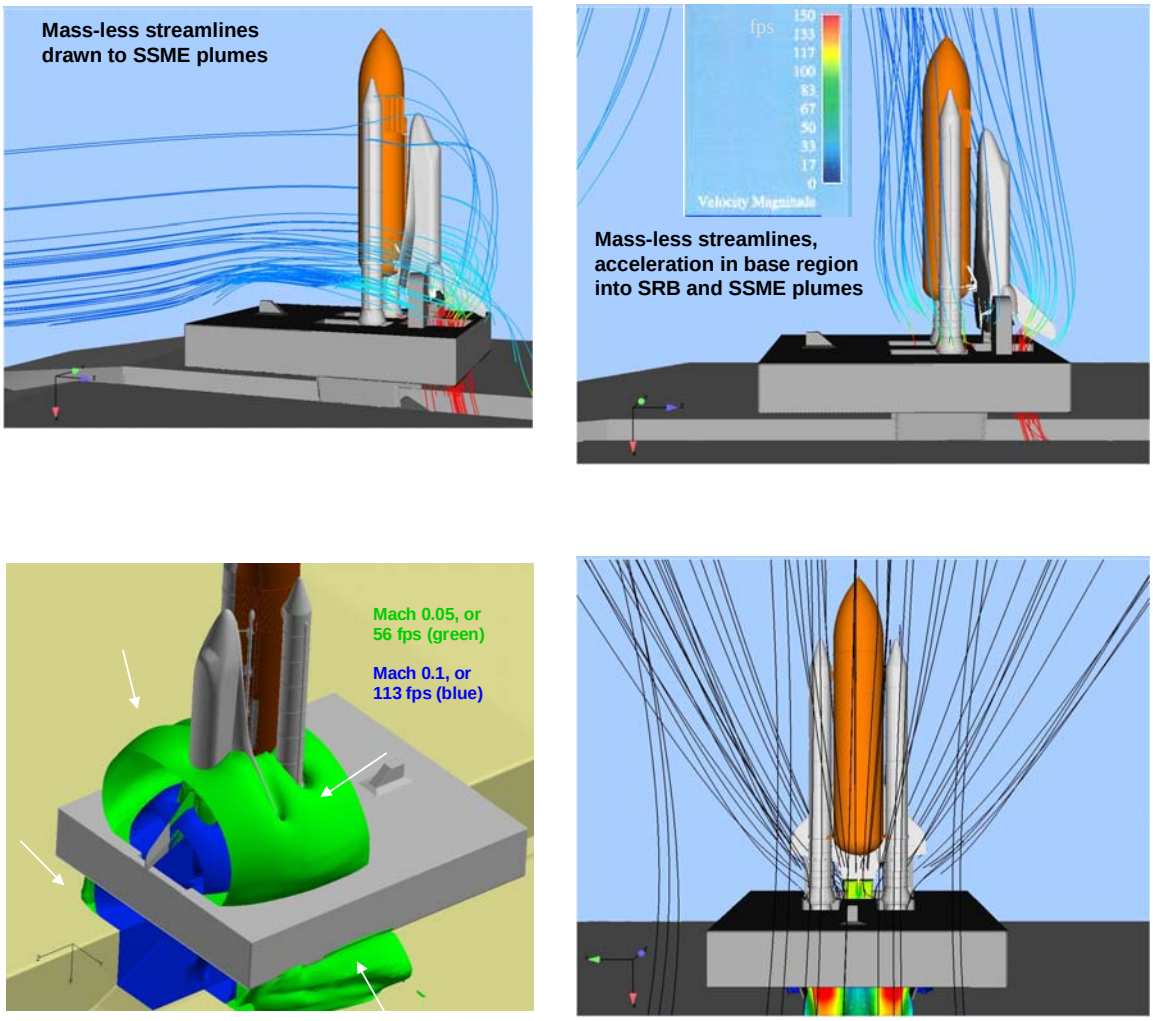

Figure 8. The 'Potential Flow' Nature of the Flow at Lift-Off

supersonic core. The view on the upper right shows details of the SRB holddown structure inside the SRB exhaust hole. The surfaces of the four holddown posts and support haunches are colored by the computed plume impingement pressure. The impingement pressure is 23 psi or more on the north holddown posts and haunches (red) as a result of the SSLV northerly drift.

The flat surfaces of the haunches below the SSLV provide particle recirculation and rebound surfaces and the side walls provide possible surfaces for particle ricochet back upwards toward the SSLV. This flow condition, which begins at ~ T0 + 1.5 sec and persists well past ~ T0 + 3 sec and up to ~ T0 + 4 sec, is therefore a critical time for the potential upward transport of liberated debris particles. The SRB plume impingement effect causes upward flow pockets with as great as 650 fps upward velocity maximum found (colored regions > 50 fps illustrated) around the South corners of the SRB Exhaust Holes and on the TSM North faces, beneath the Orbiter, and at the center of MLP Deck 0, beneath the ET. These pockets are illustrated in the bottom right corner of Figure 9. The image on the bottom left hand corner of Figure 9 shows that the SRB plumes have not yet begun to spill out of the SRB Holes on the MLP deck.

There is a change in the nature of the flow field beginning at ~ T0 + 3 sec. The SRB plumes grow in diameter with increasing distance from the nozzle exit plane and they begin to spill out of the SRB exhaust holes and onto the MLP Deck. This flow condition is illustrated in Figure 10, which is the flowfield at ~ T0 + 3 sec. The SSLV height is ~ 67 ft and the drift ~ 7 ft at this time and the SSLV has attained ~ 48 fps forward flight velocity and corresponds to CardPt 6.

At the upper left in Figure 10 is the same plume flow plus streamlines view as before, but the streamlines spill outward around the plume periphery onto the MLP Deck. There are significant horizontal components of the flow out across the Deck as seen in the view from above at the lower left. On the upper right, the plume impingement pressure (red) covers a larger surface area on the holddown posts and haunches and will lessen as the SSLV continues to climb.

The pockets of upward flow > 50 fps are smaller and it can be seen that the plume spillage causes horizontal vectors causing the flow recirculation to be directed more outward and away from the Vehicle direction. This is a condition of expected lessening severity for debris particle upward transport as the velocity field now tends to turn particles liberated after ~ T0 + 3 sec outward and away and the Vehicle is higher and accelerating away from the threat of upward-traveling debris.

CardPt 6a flowfield views are shown in Figure 11. Plume flow cross-section cuts are shown in the upper left and upper right views. The color contours are Mach number in the plumes, highest in the SSME plumes. The upper view in the center shows mass-less streamlines colored by density going from free-stream (red) to the SSME plume boundaries (blues) and indicating the very strong aspiration into the Orbiter base region. The indication is that debris particles drawn toward the base will tend to be drawn to highest velocities at the body flap, elevons, and the SSME nozzle bells.

The view at the lower left in Figure 11 shows a typical set of liberated debris particle hit locations from the ***debris*** and ***dprox*** codes run with the CardPt 6 CFD flowfield. The debris particles may have come from above or from below to result in impacts at these locations on the Orbiter.

The view at the lower right in Figure 11 shows velocity contours in a transverse cut through the SSME plumes and just above the plane of the SRB nozzle exit planes. If upward-traveling debris makes it past the blockage volume of the SRB exhaust plumes, it still has to negotiate the strong aspiration down-flow of the SSME plumes to reach the Orbiter aft extremity regions from below.

These CFD results illustrate flow characteristics known to exist at launch based on the fact that they show features of the flow seen in launch film imagery and evident in burn and damage patterns left on the Facility structure after launch.

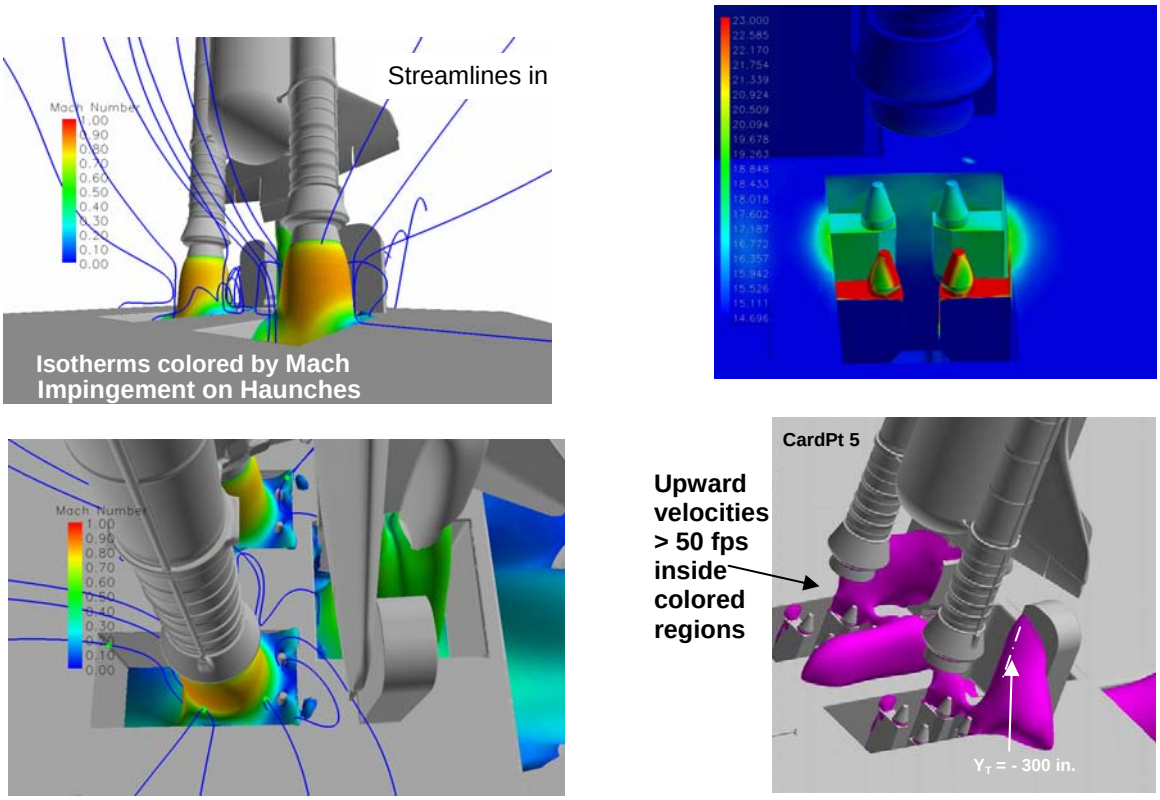

Figure 9. Cardinal Point 5.

Cycle-2 CFD Flowfield Model

The strong interactions of the SRB plumes with the SRB holddown posts, resulting in upward flow primarily motivated a follow-on effort to refine the fidelity of the CFD model. This effort has been termed the Cycle-2 Lift-off Debris Transport Analysis effort and has been underway since the beginning of Fiscal Year 2006. The Cycle-2 effort includes improvements in all aspects of the debris transport analysis; the CFD-model related improvements will be briefly discussed here.

It is still necessary to make Simplification 1 in the Cycle-2 effort. However, Simplification 2, the use of air as the plume effluent, can be improved drastically. We have chosen to use the Loci-CHEM CFD program[20, 21], one of the production-mode CFD tools at NASA/MSFC. This choice allows the SSME plume to be simulated with a quite realistic effluent and using a second order spatially accurate algorithm. Eulerian and Lagrangian-based particle flow models are being implemented to model the SRB internal and plume flows and will be available soon for use in the Cycle-2 effort to add the SRB condensed-species.

It is Simplification 3, the geometry simplification, which is receiving the most attention. The Loci-CHEM CFD program uses unstructured grids, which makes the construction of grids for complicated, detailed geometry much easier. Figure 12 shows the detail of the SRB exhaust hole and holddown posts available in the CAD model, the Cycle-1 CFD model and the Cycle-2 CFD model. The SRB-holddown post interactions will be investigated by decoupling the SRB plume

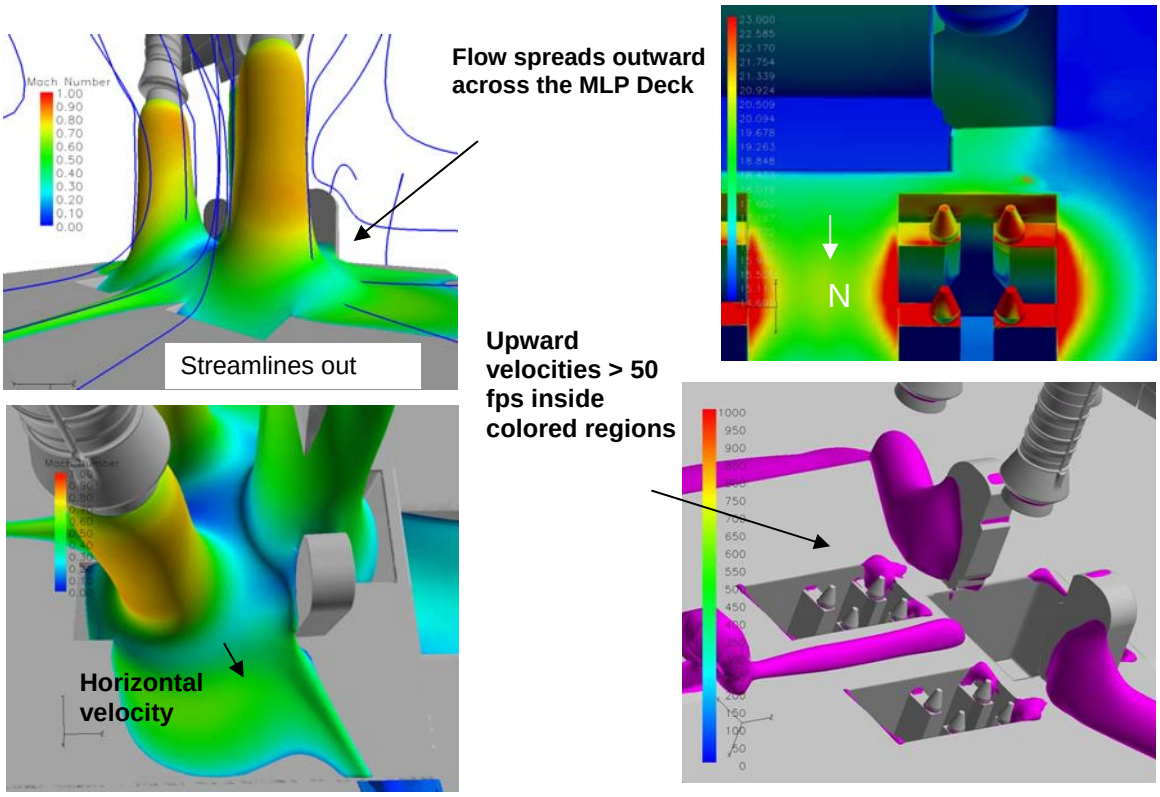

Figure 10. Cardinal Point 6.

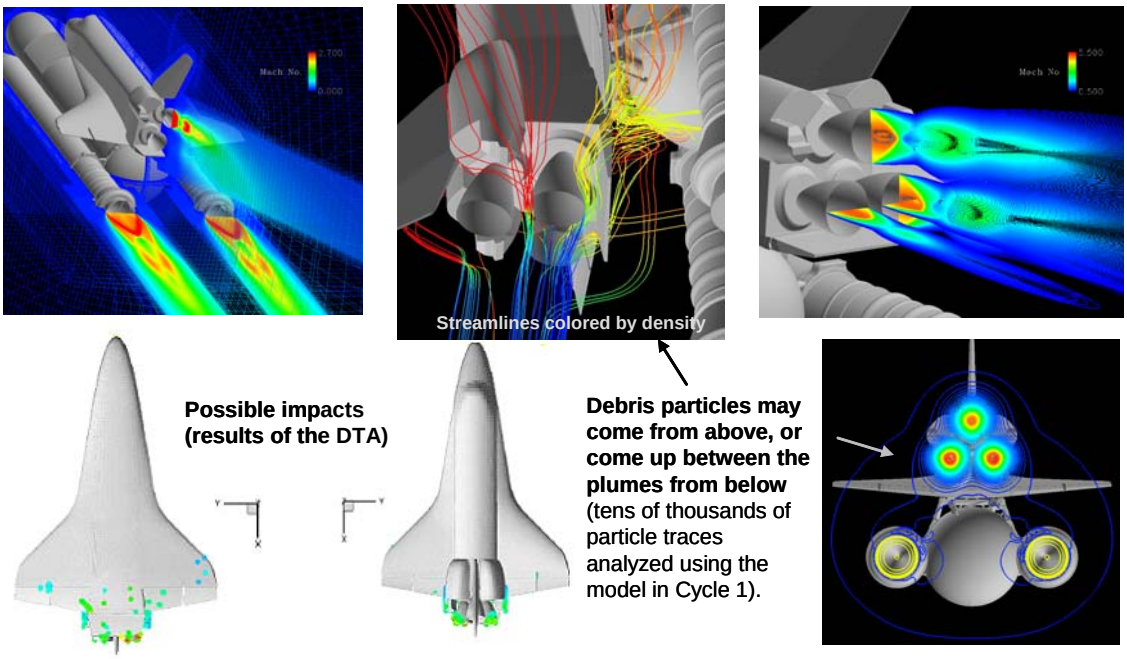

Figure 11. Vehicle Climb-out Solutions in the Timeframe after ~ T0 + 3 sec

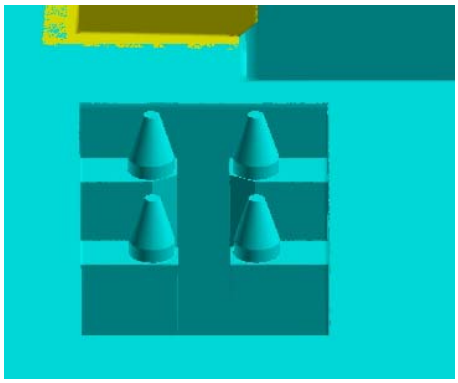

Cycle-1

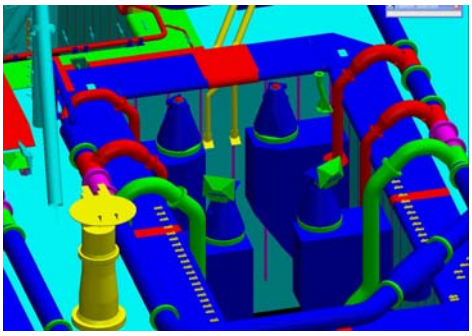

CAD Model

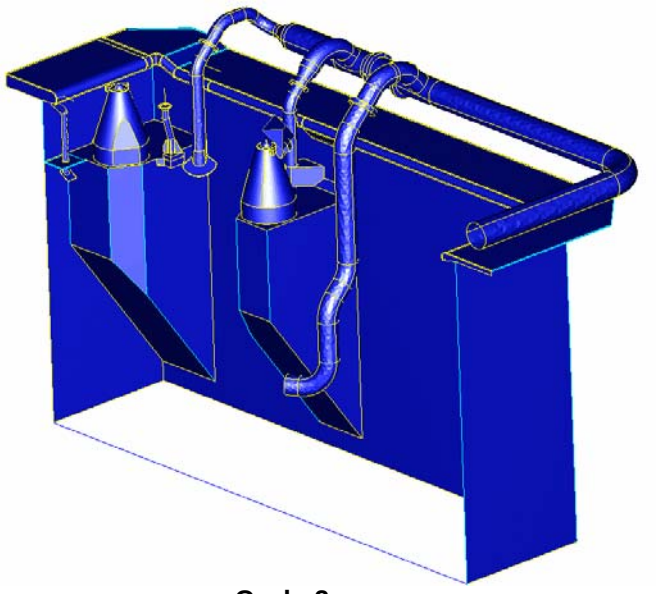

Cycle-2

Figure 12. Improvements to the SRB exhaust hole geometry

and SRB Ground model from the rest of the SSLV and Ground Facility. In this manner the recirculating and upward flow predicted from the Cycle-1 model in Figures 9 and 10 will be assessed using significantly higher fidelity physical and geometrical models.

Recently, the Loci-CHEM program has been upgraded to support real fluid equations of state, which allows the modeling of the Ignition Overpressure and Sound Suppression Water flows (see e.g. References 22 and 23). The use of this new capability will be attempted as part of the Cycle-2 effort to address Simplification 4.

Summary and Conclusions

For the first time, a comprehensive CFD model of the SSLV during Lift-Off has been constructed and executed. This CFD model contains a detailed model of the SSLV and couples it with a detailed model of the MLP, Flame Deflector, and Exhaust Trench, and Ground geometry. In addition, the effect of the wind environment has been captured by evaluating three wind velocities every 45 degrees around the compass. The wind environment and plume aspiration effects have been coupled to arrive at a prediction of the flow field through which potential debris trajectories are integrated. Over 60 CFD simulations have been completed in Cycle-1 with hundreds of debris simulation cases run with tens of thousands of potential debris transport

trajectories generated. The knowledge of the nature of the interactions of the plume-generated flow field with the Ground geometry has been used to further focus potential FOD removal and mitigation. In particular, the identification of high speed upward flow, capable of driving debris upwards towards the SSLV with significant velocities, has been identified. The Cycle-1 debris database has been built for expected debris and is being used for Day of Launch real-time mission support. A basis for real time mission decision support has been gained as a result of knowledge from the Lift-Off CFD flowfield analysis.

The Cycle-2 effort, largely motivated by the potential for driving debris upward towards the SSLV, is now under way. Cycle-2 systematically addresses the Simplifications required for the construction of the Cycle-1 CFD model. In particular, the fidelity of the plume simulation details and the fidelity of the Ground geometry from which the interaction of the SRB plumes cause the upward flow have been increased.

References

1. Columbia Accident Investigation Board Report Volume I, August 2003.

2. Gomez, R.J., Vicker, D., Rogers, S.E., Aftosmis, M.J., Chan, W.M., Meakin, R., and Murman, S., "STS-107 Investigation Ascent CFD Support," AIAA 2004-2226, July 2004.

3. Murman, S., Aftosmis, M.J., and Rogers, S.E., "Characterization of Space Shuttle Aerodynamic Debris Aerodynamics using CFD Methods," AIAA 2005-1223, January 2005.

4. Buning, Pieter, et al, "OVERFLOW Users Manual, version 2.0s," April 2003.

5. "Space Shuttle Expected Debris Generation and Impact Tolerance Requirements, Groundrules, and Assumptions," NSTS 60559, Rev A, June 30, 2006.

6. "Debris Tracking Program User's Manual v0.7.2", October 2004.

7. Rogers, Stuart, "DPROX v0.7.2," NASA Advanced Supercomputing Division, NASA Ames Research Center, 2005.

8. Dougherty, N.S., O'Farrell, J.M., and Liu, B.L., "TIDDB Verification Document Chapter 6.2 CFD Simulation 2D Views, 51L Simulation using the USA Code," 1987, for "Space Shuttle Program Thermal Interfaces Design Data Book Performance Enhancement Super Light Weight Tank", Rockwell International Space Systems Division SSD97D0271A, January, 2002.

9. Dougherty, N.S., O'Farrell, J.M., and Liu, B.L., "LCC Update CFD Solutions, 3-D ET-SRB Lower Half Model, USA Code, for Rockwell International Space Systems Division TIDDB Verification Update" 1993.

10. Chakravarthy, S. R., Szema, K-Y., Goldberg, U.C., and Gorski, J.J., "Application of a New Class of High Accuracy TVD Schemes to the Navier-Stokes Equations," AIAA 85-0165, January 1985.

11. Custodio, J.N., “Post Test Report for Space Shuttle Vehicle (SSV) Ground Winds Wind Tunnel Test IA346 (NAART105),” Boeing Report No. SI-02-078, May 21, 2002.

12. Orbiter Operational Aerodynamic Data Book,” United Space Alliance Reusable Space Systems RSS99D0001," April 2000.

13. “Performance Enhancement Operational Aerodynamic Design Data Book, Launch Vehicle Aerodynamic Data,” Boeing Reusable Space Systems RSS98D0313, January 1999.

14. Smith, Sheldon, “Unified Test Stand Design and Environmental Impact Model**,** Final Report Contract NAS13-01006,” July 2003.

15. Slotnick, J.P., Kandula, M., Buning, P., and Martin, F.W., “Numerical Simulation of the Space Shuttle Launch Vehicle Flow Field with Real Gas Solid Rocket Motor Plume Effects,” AIAA-93-0521, Reno, Nevada, January 11-14, 1993.

16. Wang, T-S., “Multidimensional Unstructured-Grid Liquid Rocket-Engine Nozzle Performance and Heat Transfer Analysis,” Journal of Propulsion and Power, AIAA, Vol. 22, No.1, January-February 2006.

17. Melton, J., NASA/KSC Launch Complex 39 CAD Model, 2004.

18. Bayyuk, Sami, “Targeted Evaluation of the Pre-conditioning in OVERFLOW 2.0s,” CFDRC Report, April 2004.

19. Spalart, P.R., and Allmaras, S.R., “A One-Equation Turbulence Model for Aerodynamic Flows,” AIAA 92-0439, January 1992.

20. Luke, E. A., and George, T., “Loci: A Rule-Based Framework for Parallel Multi-Disciplinary Simulation Synthesis,” under consideration for publication in the Journal of Functional Programming, 2005.

21. Westra, Doug, “Use, Assessment, and Improvement of the Loci-CHEM CFD Code for Simulation of Combustion in a Single Element GO2/GH2 Injector and Chamber, TFAWS 2006, College Park, MD, August 2006.

22. Pavish, D.L., and Deese, J.E., “CFD Analysis of Unsteady Ignition Overpressure Effects on Delta II and Delta III Launch Vehicles,” AIAA 200-3922, August 2000.

23. Sulyma, P.R., Carter, R.C., Audeh, B., and Smith, S.D., "Prediction of Launch Induced Thermal and Pressure Environments to Launch Complex 39, Lockheed Missiles and Space Report LMSC-HREC TR D496999, September 1976.

Nomenclature

BET Best Estimated Trajectory (of the Vehicle at Lift-off, reconstructed from flight data)

BN Ballistic number (of a debris particle), = $m/C_D A_{ref}$

CFD Computational Fluid Dynamics

C_D Drag coefficient (of a debris particle)

c_p Pressure coefficient = $(p_{local} - p_{inf})/q_{inf}$

DTA Debris Transport Analysis

ET External Tank

FOD Foreign object debris

FSS Fixed Service Structure

γ Ratio of specific of heats of gas species (ideal gas assumption)

IEEE Institute of Electrical and Electronics Engineers

JANNAF Joint Army Navy Air Force

MLP Mobile Launch Platform

MW Molecular weight (of plume gas species)

PAL Protuberance Air Load (on the ET)

Pc Chamber pressure (of the SSME and the RSRM), psia

p Static pressure, psia

q Dynamic pressure, psi

RSRM Reusable Solid Rocket Motor

Re Reynolds number

SRB Solid Rocket Booster

SSLV Space Shuttle Launch Vehicle

SSME Space Shuttle Main Engine

σ Standard deviation

T0 Time of SRB Ignition Command

TSM Tail Service Mast

t Time (in a given launch trajectory as measured from T0)

X_T Shuttle Tank axial codinate (positive going aft)

Y_T Shuttle Tank lateral coordinate (positive out RH Wing)

Z_T Shuttle Tank vertical coordinate (positive out Vertical Tail)

y^+ Non-dimensional height in the turbulent wall boundary layer on a surface

Subscripts

i	Sequence of Cardinal Point Cases (given Vehicle trajectory, given Ground Wind condition)
j	Particular flight trajectory (Vehicle climb-out)
inf	Conditions at infinity (far field)